HHS Public Access

Author manuscript

Nat Phys. Author manuscript; available in PMC 2011 December 01.

Published in final edited form as:

Nat Phys. 2011 June 1; 7(6): 508–514. doi:10.1038/nphys1936.

Random walk with barriers

Dmitry S. Novikov[1,*], **Els Fieremans**[1], **Jens H. Jensen**[1,2], and **Joseph A. Helpern**[3]

[1] Center for Biomedical Imaging, Department of Radiology, New York University School of Medicine, New York, NY 10016, USA

[2] Department of Physiology and Neuroscience, New York University School of Medicine, New York, NY 10016, USA

[3] Department of Radiology and Radiological Science, Medical University of South Carolina, Charleston, SC 29425, USA

Abstract

Restrictions to molecular motion by barriers (membranes) are ubiquitous in porous media, composite materials and biological tissues. A major challenge is to characterize the microstructure of a material or an organism nondestructively using a bulk transport measurement. Here we demonstrate how the long-range structural correlations introduced by permeable membranes give rise to distinct features of transport. We consider Brownian motion restricted by randomly placed and oriented membranes ($d-1$ dimensional planes in d dimensions) and focus on the disorder-averaged diffusion propagator using a scattering approach. The renormalization group solution reveals a scaling behavior of the diffusion coefficient for large times, with a characteristically slow inverse square root time dependence for any d. Its origin lies in the strong structural fluctuations introduced by the spatially extended random restrictions, representing a novel universality class of the structural disorder. Our results agree well with Monte Carlo simulations in two dimensions. They can be used to identify permeable barriers as restrictions to transport, and to quantify their permeability and surface area.

Brownian motion in a uniform medium is characterized by a single parameter, the diffusion coefficent D, which is a measure of mean square molecular displacement. A packet of random walkers spreads with time t according to a Gaussian distribution with variance $\langle x^2 \rangle = 2Dt$. Complexity in the microscopic structure of a sample, such as heterogeneity in diffusive properties and restrictions to molecular motion, results in non-Gaussian evolution1,2. In particular, diffusion becomes dispersive, leading to the time-dependence of the diffusion coefficient $D(t)$.

---

[*]Correspondence and requests for materials should be addressed to D.S.N. (dima@alum.mit.edu).

Author contributions

D.S.N. performed analytical calculations and wrote the manuscript. E.F. performed numerical calculations. All authors discussed the results and implications and commented on the manuscript at all stages.

Additional information

The authors declare no competing financial interests.

A fundamental question is how specific complexity features manifest themselves in the dispersive dynamics. Random drifts are known to drastically slow the dynamics down to $\langle x^2\rangle \sim \ln 4\, t$, thereby suppressing the diffusion, $D|_{t\to\infty} = 0$, in one dimension3,4. Their effect in higher dimensions is less profound5–9. Short-range disorder in local diffusion coefficient preserves Gaussian diffusion for $t \to \infty$, resulting in the finite macroscopic diffusion constant $D_\infty \equiv D(t)|_{t\to\infty}$. However, it causes a long-time tail10,11 in the velocity autocorrelator $\mathcal{D}(t) = \langle v(t)v(0)\rangle \sim t^{-(d+2)/2}$, with the power-law exponent depending on the spatial dimensionality d. Equivalently, the diffusivity $\mathscr{D}(\omega)=\int_0^\infty dt\, e^{i\omega t}\mathscr{D}(t) \simeq D_\infty + \mathrm{const}\cdot\omega^{d/2}$ acquires non-analytic dispersion at low frequencies10,11. Studying dispersive diffusion, therefore, is a way to characterize the type of disorder and of restrictions to molecular motion in a complex sample.

Here we consider a novel class of restrictions to diffusion, represented by extended barriers (membranes). Practically, membranes regulate the transport of ions12, water molecules13–16 and gases17 in biological tissues18. Permeable barriers may partition cell membranes, modulating phospholipid motion19–21. Barriers also restrict molecular motion in porous and composite materials22–27. On a fundamental level, extended barriers may introduce significant long-range correlations into the sample structure. We show that these correlations give rise to distinct transport features, qualitatively different from those due to short-range disorder which is a default assumption in the models of transport10,11,28.

We develop a minimal model of a d-dimensional medium with spatially extended disorder, assuming that diffusion is restricted by randomly placed and oriented infinite flat membranes with a given permeability, such as in the $d = 2$ example of Fig. 1. Based on the renormalization group analysis, we find an accurate approximation for the diffusion coefficient as a function of time or frequency, for all membrane concentrations and permeabilities, as confirmed numerically for $d = 2$ in Fig. 2.

Remarkably, the spatially extended disorder introduced by the membranes in any d results in a long-term memory, that manifests itself in the long-time tail $\mathcal{D}(t) \sim t^{-3/2}$ in the velocity autocorrelator (Fig. 3); in a non-analytic dispersive diffusivity $\mathcal{D}(\omega) \simeq D_\infty + \mathrm{const}\cdot\omega^{1/2}$ at low frequencies; and in a characteristically slow decrease of the diffusion coefficient, $D(t) = D_\infty + \mathrm{const}\cdot t^{-1/2}$ as $t \to \infty$, Fig. 2, causing the mean square displacement to increase as $\langle x^2\rangle \simeq 2D_\infty t + \mathrm{const}\cdot t^{1/2}$. The $\omega^{1/2} \sim t^{-1/2}$ dispersive diffusion is shown to be a consequence of anomalously strong structural fluctuations in a sample with spatially extended barriers. For membranes with finite extent or correlation length r_c, the signature $\omega^{1/2}$ dispersion will switch to its short-ranged counterpart $\omega^{d/2}$ after the diffusion length exceeds r_c.

Our model represents a novel universality class of the structural disorder in classical random media. An essential feature of the $\omega^{1/2} \sim t^{-1/2}$ dispersion is that, at sufficiently long times, it dominates the short-range disorder contribution for $d > 1$. Hence, if observed, this dispersion can serve as a “fingerprint” of spatially extended restrictions within the complexity of heterogeneous samples. Practically, such a dependence can manifest itself in a variety of transport measurements, such as the electrical29 or heat conduction, or the diffusion-weighted NMR15.

Model

A membrane is an idealization of a thin slice of a poorly diffusive material, as long as its thickness is negligible compared to the shortest observable diffusion length. In the limit when both the diffusion coefficient D_m of the membrane material and its thickness l_m vanish, the ratio $\kappa \equiv D_m/l_m$ is by definition the *permeability*. The effect of a membrane is described by the boundary condition18,30

$$-\mathbf{nJ}|_{\mathbf{r}_m} = D_0 \mathbf{n}\partial_{\mathbf{r}}\psi|_{\mathbf{r}=\mathbf{r}_m} = \kappa[\psi_{\mathbf{r}_m+\mathbf{n}0} - \psi_{\mathbf{r}_m-\mathbf{n}0}]. \quad (1)$$

Here D_0 is the unrestricted diffusion coefficient. The condition (1) means that, at each point $\mathbf{r}_m$ of the membrane, the density ψ of random walkers experiences a jump proportional to the component of the current **J** along the normal **n** to the membrane surface.

The permeability has the dimensions of velocity. In what follows, we find it useful to associate an *effective thickness*, $2\ell = D_0/\kappa$, with a membrane. This length scale is defined relative to the free diffusion coefficient D_0. Its physical meaning is derived from the condition (1) and is illustrated in Fig. 3a; the membrane indeed appears $D_0/D_m \gg 1$ times thicker than its "nominal" vanishing thickness l_m.

Consider now diffusion in a macroscopic sample embedded with multiple membranes, each one imposing the condition (1). The diffusion propagator depends on their number, shape, and spatial distribution. The number of membranes is characterized by the ratio S/V of their total surface area to the sample volume. Here we adopt the convention from the porous media literature16,24: as the random walkers can approach a membrane from both faces, the membrane's surface area is counted twice in S. The shape and the spatial distribution of the membranes vary greatly depending on the physical context. The distinct dispersive features of transport due to spatially extended restrictions can be captured by making the simplest assumption which also allows us to keep the number of parameters to a minimum. Namely, below we consider the membranes as infinite $d - 1$ dimensional planes placed and oriented in a completely random (uncorrelated) way, dividing the sample into pores with random shapes, as shown in Fig. 1 for $d = 2$. In this case, the ratio S/V is all that is needed to characterize the geometry.

In what follows, we first outline our main results for the model medium. Next, we derive them, compare with numerical simulations, discuss and generalize.

Results for randomly oriented flat membranes

In the $t \to \infty$ limit, the diffusion becomes Gaussian with the reduced diffusion coefficient

$$D_\infty \simeq \frac{D_0}{1+\zeta}, \quad \zeta = \frac{S\ell}{Vd}. \quad (2)$$

Here the dimensionless parameter ζ quantifies the ability of membranes to hinder the diffusion. It is the "volume fraction" occupied by the membranes based on the effective

thickness ℓ defined above. The result for D_∞ is exact in $d = 1$, ref. 31. As follows from Fig. 2, it is a good approximation for $d > 1$, with $1/d$ in equation (2) arising from the mean-field orientational averaging, cf. Methods section. Strong restrictions correspond to $\zeta > 1$, when the domains of thickness $\sim \ell$ associated with each membrane overlap, such that transport across a membrane is affected by its neighbors.

For finite t, we shift to the frequency representation since the restrictions are stationary. Technically, we focus on the diffusion propagator G averaged over the disorder in positions and orientations of the random membranes. After disorder averaging, the propagator becomes translation invariant. Its pole in the frequency – wave vector representation, $G^{-1}_{\omega,\mathbf{q}} = -i\omega + \mathscr{D}(\omega)q^2 + \mathscr{O}(q^4)$, defines the dispersive diffusion coefficient (diffusivity) $\mathscr{D}(\omega)$ which is a retarded response function that relates the disorder-averaged particle current $\mathbf{J}_{\omega,\mathbf{r}} = -\mathscr{D}(\omega)\partial_{\mathbf{r}}\psi_{\omega,\mathbf{r}}$ to the density gradient32.

The corresponding time-dependent diffusion coefficient

$$D(t) \equiv \frac{\langle x^2(t)\rangle}{2t} = -\frac{1}{t}\int \frac{d\omega}{2\pi} e^{-i\omega t}\frac{\mathscr{D}(\omega)}{(\omega+i0)^2} \quad (3)$$

is given32 by a contour integration along the real axis with all the singularities in the lower half-plane of complex ω.

We find $\mathscr{D}(\omega)$ in three steps. First, we develop a scattering approach for the transmission events described by the boundary conditions (1) at each membrane. Second, we solve the problem perturbatively in the volume fraction ζ at the mean-field level, starting from infinitely permeable limit $\mathscr{D}(\omega) \equiv D_0$. These two steps are done in the Methods section. The resulting diffusivity

$$\mathscr{D}(\omega) = D_0\,[1 - \zeta\tilde{\phi}(\omega)], \qquad \tilde{\phi}(\omega) = \frac{1}{1 - z_\omega}, \quad (4)$$

with $z_\omega = i\sqrt{i\omega\tau}$ and $\tau = \ell^2/D_0 = D_0/(2\kappa)^2$, is exact in the limit when the correction $\zeta|\tilde{\varphi}(\omega)| \ll 1$ is small. This condition holds either for sufficiently permeable membranes, $\zeta \ll 1$, or at short times $\sqrt{D_0 t}S/V \ll 1$ for arbitrary permeability. The corresponding velocity autocorrelator $\mathscr{D}(t) = D_0\,[\delta(t) - \zeta\varphi(t)]$ contains a nonlocal in time memory kernel

$$\phi(t) = \int \frac{d\omega}{2\pi} e^{-i\omega t}\tilde{\phi} = \frac{1}{\sqrt{\pi\tau t}} - \frac{1}{\tau}e^{t/\tau}\operatorname{erfc}\sqrt{t/\tau}, \quad (5)$$

Fig. 3b, which will be discussed in detail below.

At the third step, we extend equation (4) onto the non-perturbative domain $\zeta \gg 1$ using the real-space renormalization group to account for the multiple transmission events self-consistently, as described below. Thereby we obtain our main result for all ζ,

$$\frac{D_0}{\mathscr{D}(\omega)} = 1+\zeta+2z_\omega(1-z_\omega)\left[\sqrt{1+\zeta/(1-z_\omega)^2}-1\right]. \quad (6)$$

Effective circuit

Before deriving our main result (6), we note that the perturbative limit (4) can be represented as a simple effective circuit. As the random walkers are uncharged, the current **J** has only the diffusive component, and the diffusivity $\mathcal{D}(\omega)$ defines its response to a density gradient $\partial_{\mathbf{r}}\psi$ rather than to a potential bias. With this important distinction29, the $\mathcal{O}(\zeta)$ result (4) can be viewed as an "impedance" $Z(\omega)$ of a hypercube L^d, $L^{d-2}Z(\omega) \equiv 1/\mathcal{D}(\omega) \approx 1/D_0 + nZ_m(\omega)$, which acts as a one-dimensional disordered transmission line of length L with point impedances $Z_m = \tilde{\varphi}(\omega)/\kappa$ placed at random positions in series, with density $n = S/(2V\,d)$. Adding independent contributions Z_m is tied to the Poissonian statistics in the positions of the barriers (see the sections on the origin of the $\sqrt{\omega}$ dispersion, and Methods).

In the dc limit, a membrane acts as a resistor with the "resistance" $1/\kappa \equiv Z_m(0)$; as $\zeta = 2\ell n$, each membrane effectively adds the length 2ℓ to the original clean wire L if its dc resistance were to match $Z(0) \propto 1/D_\infty$. At finite frequencies the resistor is shunted by the Warburg element33 with the "conductance" $g_W(\omega) = -\kappa z_\omega = \sqrt{i\omega D_0}/2i$ independent of the permeability. The Warburg impedance ~ $1/g_W$, first observed at a flat metal electrode in an electrolyte by Kohlrausch34 and Wien35 in the 19th century, is associated with the diffusion-limited response33. Incidentally, the impedance $Z(\omega)$ matches the empirical Cole form36,37 with power law exponent $\frac{1}{2}$.

Renormalization group

To calculate the response $\mathcal{D}(\omega)$ of the disordered transmission line for finite ζ, we employ the following scaling argument, which we first develop for $d = 1$. Consider a slab of length L with the diffusivity $\mathcal{D}(\omega)|_L$. Let us extend the slab to the length $L' = bL$, $b > 1$, and rescale; now the slab's length L' in new units is back to L, while the original, shorter slab has length $L \to L/b$. The rescaled slab conductance decreases due to adding extra $N' - N = N\delta b$ membranes, $\delta b = b - 1$. The diffusivity is then reduced as

$$\mathscr{D}(\omega)|_{L'} = \mathscr{D}(\omega)|_L \left[1 - \delta n \frac{\mathscr{D}(\omega)|_L}{\kappa - \frac{i}{2}\sqrt{i\omega\mathscr{D}(\omega)|_L}}\right] \quad (7)$$

according to equation (4), as long as the added membrane density $\delta n = (N/L)\delta b$ is small, $\delta b \ll 1$. Since we assumed from the beginning that the membrane positions are uncorrelated, adding a small number of membranes in an uncorrelated way at each step is consistent. Choosing an infinitesimal $dn \propto db$, we represent equation (7) in the differential form, obtaining the real-space renormalization group (RG) equation

$$\frac{d\mathscr{D}(\omega)}{dn} = -\frac{\mathscr{D}^2(\omega)}{\kappa - \frac{i}{2}\sqrt{i\omega\mathscr{D}(\omega)}}. \quad (8)$$

This is a telegraph equation for a disordered transmission line. Equivalently, it can be obtained by adding membranes in small increments δn in a macroscopic sample of a fixed length with bare diffusivity D_0, and applying the relation (4), treating all previously added membranes in the effective-medium fashion38–40 at each RG step. The diffusivity thus decreases as long as $\kappa < \infty$. In d dimensions, rescaling a hypercube L^d as in ref. 41 is equivalent to rescaling a $d = 1$ slab in which the effective one-dimensional membrane concentration $n = S/(2Vd)$. At the mean-field level, the problem is always one-dimensional, with the fraction $1/d$ of membranes exerting full resistance.

Integrating equation (8) yields our main result (6). In the dc limit $\mathscr{D}(0) \equiv D_\infty$, the RG flow $1/D_\infty|_{L'} = 1/D_\infty|_L + (N' - N)/(\kappa L d)$ recovers the above exact result (2) for $d = 1$, if one identifies L with the microscopic scale such that $D_\infty|_L \equiv D_0$ (the bare diffusivity) and $(N' - N)/Ld \to n$, the final membrane density. Written as RG flow, however, the evolution of the diffusivity is not tied to a particular microscopic cutoff; indeed, the diffusivity $D_\infty|_L$ can itself originate from "more microscopic" membranes on the scale finer than L, and so forth.

We also note an interesting equivalent way of looking at the RG flow: Formally identifying the particle number density ψ entering the diffusion equation with an electrostatic potential, the dc limit corresponds to the electrostatic screening of the one-dimensional electric field (the slope $\partial_x\psi$) by the dipoles (membranes acting as double layers). Coarse-graining corresponds to more dipoles contributing to the screening42, which renormalizes the effective dielectric constant, $1 \to 1 + \zeta$.

Regimes for $D(t)$ and numerical simulations

Consider first the most general case, which corresponds to the strong disorder, $\zeta \gg 1$. In this case, there are three distinct regimes in $D(t)$, Fig. 2, separated by the two time scales, $\tau_r \gg \tau_D$, defined below.

The initial decrease of the diffusion coefficient

$$D(t) \simeq D_0\left[1 - \frac{S}{Vd}\left(\frac{4\sqrt{D_0 t}}{3\sqrt{\pi}} - \kappa t\right)\right] \quad (9)$$

exactly reproduces the well-known universal short-time $\sqrt{t}$-expansion24. The correction to free diffusion arises from the random walkers within the diffusion length $\sim \sqrt{D_0 t}$ from the barriers; the term $\propto t$ is the permeability effect27 of flat pore walls. The limit (9) is valid as long as only a small fraction of random walkers has encountered the barriers, i.e. for $t \ll \tau_D$, where $\tau_D = \bar{a}^2/2D_0$ is the diffusion time across the typical pore size $\bar{a} \simeq 1/n = 2Vd/S$. Equation (9) follows already from the perturbative limit (4) universally valid for high frequencies, $\omega\tau_D \gg 1$. It corresponds to the $t \ll \tau$ limit of the memory kernel (5), Fig. 3b,

exemplifying negative velocity autocorrelation near a wall43, which diverges as $t^{-1/2}$ at short t. There is a perfect agreement between theory and simulations in this regime for all ζ.

Highly restrictive membranes look completely impermeable for $t \ll \tau_r$, where $\tau_r = V/(\kappa S)$ is the residence time18 within a typical pore; in our notation, $\tau_r = (\zeta/d)\,\tau_D$. As a result, the mean square displacement $\langle x^2 \rangle$ is bounded by $\sim \bar{a}^2$, and $D(t)/D_0 \sim \tau_D/t$. For our RG result (6), the "impermeable" behavior occurs for $1 \ll \sqrt{\zeta} \ll |z_\omega| \ll \zeta$, and yields the purely imaginary ζ-independent limit $\mathcal{D}(\omega) \simeq -i\omega\bar{a}^2$ (similar to the purely reactive electrical conductivity), corresponding to $D(t)/D_0 \simeq 2\,\tau_D/t$, or, equivalently, to $D(t)/D_\infty \simeq 2d\ \tau_r/t$, Fig. 2b. Both our result (6) and the simulations display the $1/t$ dependence for $\zeta \gtrsim 100$, with the theory somewhat overestimating the $D(t)$ obtained from the numerics for very large ζ (as discussed in the Methods section).

For times longer than τ_r, the system becomes aware of the finite leakage across the membranes, with $D(t)$ approaching the limit (2) which can be qualitatively estimated as hopping on a d-dimensional lattice with a step $\bar{a}$ over the time τ_r, $D_\infty \sim \bar{a}^2/(\tau_r d)$.

Remarkably, the way $D(t)$ approaches D_∞ slows down from $1/t$ to $1/\sqrt{t}$-decrease in any dimensionality d, defining the novel disorder universality class:

$$D(t) \simeq D_\infty \left(1 + C_d(\zeta)\sqrt{\frac{\tau_r}{t}}\right), \quad t \gtrsim \tau_r. \quad (10)$$

This follows in our model (6) from $D(\omega) \simeq D_\infty[1 - C_d(\zeta)\cdot i\sqrt{i\pi\omega\tau_r}/2]$ in the limit $|z_\omega| \ll \sqrt{\zeta}$, with $C_d(\zeta) = C_d(\infty)\sqrt{\zeta}(\sqrt{1+\zeta} - 1)/(1+\zeta)$ and $C_d(\infty) = \sqrt{8d/\pi}$. The regime (10) can be clearly seen from the simulation results of Fig. 2b where time is in the units of τ_r for a set of permeabilities. In this limit, the relative deviation $[D(t) - D_\infty]/D_\infty \lesssim 1$. We emphasize that for $\zeta \to \infty$, the dependence (10) approaches a universal scaling law with a fixed $C_d = C_d(\infty)$, which can be represented only in terms of the effective parameters D_∞ and τ_r, independent of the original microscopic parameters D_0, κ and S/V. Approaching this law corresponds to the collapse of the simulation curves in Fig. 2b onto one universal curve for $\zeta \gtrsim 100$ and $t \gtrsim \tau_r$. Our RG approximation (6) overestimates the $C_2(\infty)$ obtained from the fit of the numerical curves to equation (10), as illustrated in Fig. 2c. For finite ζ, the parameters $C_d(\zeta)$ and D_∞ [equation (2)] agree with the simulations within about 15% and 30% correspondingly, even in the strongly non-perturbative regime of $\zeta \gtrsim 100$. For the moderate disorder, $\zeta \sim 1$, the agreement between theory and simulations is very good.

The fact that the RG solution works fairly well even when the "small parameter" $\zeta \gg 1$ can be understood in terms of the flow to the moderately disordered limit with strongly renormalized parameters, $D_0 \to D_\infty$ and $\tau \to \tau_r$. Indeed, for $t \gg \tau_r$, the medium effectively looks as if it had a decreased diffusion coefficient D_∞. This, in turn, reduces the contrast between the diffusion coefficient inside the membrane and of its surroundings, effectively changing $D_0 \to D_\infty$ in the boundary condition (1), thereby reducing the effective thickness $\ell \to \tilde{\ell} = D_\infty/(2\kappa) \simeq \ell/\zeta \sim \bar{a}$ down to the mean distance between membranes. Hence, the renormalized disorder strength is reduced, $\zeta \to \tilde{\zeta} \equiv S\tilde{\ell}/Vd \sim 1$. Likewise, the renormalized

time scale $\tau \to \tilde{\tau} \equiv \tilde{\ell}^2/D_0 \sim \tau_r$ matches the residence time. At this point the perturbative limit (4) is matched.

Conversely, when the membranes are highly permeable, $\zeta \ll 1$, the residence time in a pore is of the order of τ_D, and the time scale τ_r defined above becomes obsolete. In this limit, our result (4) becomes exact, the intermediate $1/t$ regime does not appear, and the short-time behavior (9) directly crosses over to the nonanalytic dispersion of the form (10),

$$D(t)|_{t\gg\tau} \simeq D_\infty \left(1+\frac{2\zeta}{\sqrt{\pi}}\sqrt{\frac{\tau}{t}}\right), \quad \zeta \ll 1, \quad (11)$$

which follows from the expansion of $C_d(\zeta)$ using $\tau = \zeta(d/2)\tau_r$, and corresponds to the $t \gg \tau$ limit of the kernel (5), Fig. 3b.

Origin of the $\sqrt{\omega} \sim 1/\sqrt{t}$ dispersion

Consider first the perturbative $\zeta \ll 1$ limit, which already contains the necessary physics. Here the two important time scales are τ_D and $\tau = \frac{1}{2}\zeta^2\tau_D$. We first focus on the case $t \ll \tau_D$, where adding independent contributions, as done in the Effective circuit and Methods sections, is justified since multiple scatterings off different membranes are not yet important. In this case, the dispersive behavior (11) for $\tau \ll t \ll \tau_D$ is a result of scattering off individual barriers. As described in the Methods section, it represents slow density equilibration across a barrier, following the $t^{-1/2}$ decrease of the probability of a random walker to never return to the origin.

For longer times $t \gg \tau_D$, multi-barrier scatterings determine the time dependence of $D(t)$ which becomes sensitive to spatial correlations between membranes. Indeed, by the time t, the medium is effectively *coarse-grained* into domains of the size $\sim L(t) = \sqrt{2Dt} \gg \bar{a}$. These domains have slightly different diffusion coefficients D_j due to a different amount of restrictions falling into them as a result of the disorder. The net diffusion coefficient $D(t) \equiv \langle D_j \rangle$ is the ensemble average over the domains; in d dimensions, $D(t) \simeq D_\infty + \langle(\delta D_j)^2\rangle / dD_\infty$, where $\delta D_j = D_j - \langle D_j \rangle$. The distribution variance $\langle(\delta D_j)^2\rangle \sim 1/L^d(t)$ scales inversely with the domain volume for the short-range disorder due to the Poissonian statistics, yielding the $\omega^{d/2} \sim t^{-d/2}$ dispersion10,11,44–46. This disorder effect should be contrasted with the much faster decrease of $D(t)$ and $\mathcal{P}(t)$ in the absence of spatial fluctuations, both for the strictly periodic barriers in d = 1,47,48 and for the single-scale dominated disorder in any d, ref. 32.

Remarkably, the spatially extended disorder introduced in this work produces qualitatively *stronger* fluctuations in the coarse-grained distribution of $\{D_j\}$, with the variance $\langle(\delta D_j)^2\rangle \sim 1/L(t)$ decreasing much slower than $1/L^d(t)$ in $d > 1$. This signature scaling in fact holds for any ζ, resulting in the $\omega^{1/2} \sim t^{-1/2}$ dispersion as long as $L(t) \gg \bar{a}$, both for $t \gg \tau_D$ (when $\zeta \ll 1$) and for $t \gg \tau_r$ (when $\zeta \gtrsim 1$). To see this, one can first assume the membranes oriented normal to the orthogonal basis vectors (with otherwise random positions). In this basis, the eigenvalues of the isotropic diffusion tensor correspond to the d = 1 disorder, with the scaling $\langle(\delta D_j)^2\rangle \sim 1/L(t)$ due to the Poissonian disorder along each basis direction,

effectively bringing us back to the $d = 1$ case10,11,44–46. The observed $\omega^{1/2} \sim t^{-1/2}$ dispersion attests to the fact that tilting each membrane in a random direction (Fig. 1) does not qualitatively alter this scaling.

Finally, we note that the above single-barrier and coarse-graining pictures are equivalent for our model, i.e. the connection with the return-to-origin probability can be formally extended onto $t \gg \tau_D$ or $t \gg \tau_r$, by substituting the rest of the system via a "featureless" effective medium with diffusivity D_∞. Indeed, by adopting the lattice calculation44 to barriers randomly placed on a line, we observe that the prefactor $C_1(\zeta)$ for $\zeta \ll 1$, and, with it, equation (11), is exact in $d = 1$. This means that, for $\zeta \ll 1$, adding independent barrier contributions in a mean-field way (4) is fully compatible with the Poissonian statistics of the disorder for $L(t) \gg \bar{a}$. For finite ζ, the equivalence between the Poissonian disorder in barrier positions and the return-to-origin probability persists in the RG solution, as it is utilized at every RG step (7). As a result, these two pictures remain equivalent even in the $\zeta \gg 1$ limit, after the effective-medium substitution $\tau \to \tau_r$, yielding the scaling behavior (10) for all ζ and t.

Outlook

In this work we have introduced a novel disorder class, the extended disorder, represented by straight permeable membranes which are randomly placed and oriented. A random medium of this type has dispersive diffusion $\mathcal{D}(\omega) = D_\infty + \text{const} \cdot \omega^{1/2}$ in any dimensionality d as a result of anomalously strong structural fluctuations. According to the coarse-graining argument, any medium with extended structural blocks (e.g. infinite membranes with finite thickness) falls into this class.

The $\omega^{1/2}$ dispersion for $d > 1$ is notably more singular than its well studied $\omega^{d/2}$ counterparts arising due to short-range disorder10,11. As the $\omega^{1/2}$ singularity originates from long-range spatial correlations introduced by the membranes, the dispersive behavior of the form (10) will persist in a variety of samples with random extended restrictions, and will become increasingly important for longer diffusion times when the contributions from short-range disorder components vanish. However, the behavior (10) will eventually terminate if the membranes cease to be extended past their intrinsic correlation radius r_c, i.e. for $t > t_c \sim r_c^2/D(t_c)$, when the structural memory is forgotten, and the short-range dispersion $\omega^{d/2}$ of a coarse-grained random medium sets in.

Methods

A single barrier in one dimension

The boundary condition (1) can be represented as a local scattering term in the diffusion equation

$$\partial_t \psi = D_0 \partial_x^2 \psi + \hat{V}_x \psi, \quad \hat{V}_x \psi \equiv -2 D_0 \ell \delta'(x) \left[\partial_x \psi\right]_{x=0}. \quad (12)$$

Here $\delta'(x)$ is the derivative of the Dirac delta-function at the position $x = 0$ of the membrane.

We focus on the Green's function $\mathcal{G}_{t;x,x'}$ of the problem (12), defined by the initial condition $\mathcal{G}_{t;x,x'}|_{t=0} = \delta(x - x')$. As the problem is stationary, we shift to the frequency domain, $\partial_t \to -i\omega$. In this representation, the Green's function $\mathcal{G}_{\omega;x,x'}$ is formally an operator inverse

$$\mathscr{G}_\omega = \left[G_\omega^{(0)^{-1}} - \hat{V} \right]^{-1} \quad (13)$$

where the coordinates x play a role of indices in infinite-dimensional matrices, and the free propagator

$$G^{(0)}_{\omega,q} = \frac{1}{-i\omega + D_0 q^2}. \quad (14)$$

The result of inversion (13) is the Born series

$$\mathscr{G}_{\omega;x,x'} = G^{(0)}_{\omega;x-x'} + \int dx_1 G^{(0)}_{\omega;x-x_1} \mathbf{V}_{\omega;x_1} G^{(0)}_{\omega;x_1-x'} \quad (15)$$

where the exact vertex $\mathbf{V}$ (the T-matrix) satisfies the Dyson's equation, which in the Fourier representation reads

$$\mathbf{V}_{\omega;k,k'} = V_{k,k'} + \int \tfrac{dq}{2\pi} V_{k,q} G^{(0)}_{\omega,q} \mathbf{V}_{\omega;q,k'}. \quad (16)$$

In our case, the bare vertex is separable,

$$\hat{V} \to V_{k,k'} = 2D_0 \ell k k'. \quad (17)$$

The solution of equation (16), the exact vertex

$$\mathbf{V}_{\omega;k,k'} = \tilde{\phi}(\omega)\, V_{k,k'}. \quad (18)$$

Throughout this work, ω is understood as having an infinitesimal positive imaginary part $+i0$ due to causality; this way the retarded response functions are analytic in the upper-half-plane of the complex variable ω.

The $\omega^{1/2}$ singularity in $\tilde{\varphi}(\omega)$ parallels that of the energy-dependent quantum scattering off a localized potential $\lambda\delta(x)$ in one dimension, identifying $i\omega \to \varepsilon + i0$. In the quantum problem, however, energy comes with a negative power $\varepsilon^{-1/2}$ in the denominator of the corresponding exact vertex $\tilde{\lambda}(\varepsilon)$, so that the high-energy scattering corresponds to the Born limit $\tilde{\lambda} \to \lambda$, whereas the low-energy amplitude $\tilde{\lambda} \sim \lambda\sqrt{\varepsilon}$. For the diffusion, the Born approximation $\mathbf{V}_{\omega;k,k'} \to V_{k,k'}$ corresponds to the dc limit, whereas at high frequencies $\mathbf{V}_{\omega;k,k'} \sim V_{k,k'}/\sqrt{\omega}$, as the scope of the p barrier is reduced down to the particles within the diffusion length $\sim \sqrt{D_0/\omega}$.

Return to origin probability and impedance

The Green's function $\mathcal{G}_{t;x,x_0}$ describes the density equilibration after injecting a unit packet of random walkers at the point x_0 at $t = 0$. For $x_0 > 0$, the excess number of walkers $Q_{x_0}(t) \equiv \int_0^\infty dx\, \mathcal{G}_{t;x,x_0} - \frac{1}{2} \simeq \frac{1}{2} P_{\rm surv}(t;x_0+\ell)$ that has not yet leaked out across the barrier, asymptotically follows the survival probability $P_{\rm surv}(t;\tilde{x}_0) \simeq \tilde{x}_0/\sqrt{\pi D_0 t}$ of a particle released at a distance $\tilde{x_0} = x_0 + \ell$, to never return to the origin. This relation is valid for $t \gg \tilde{x}_0^2/D_0$, such that the resulting density gradient is uniform on either side of the barrier, and relaxes as $t^{-1/2}$, following the fraction $P_{\rm surv}(t, \tilde{x_0})$ of the walkers who have managed to wander around the "biased" side ($x > 0$) and have not yet encountered the barrier. The finite permeability κ in this picture is substituted by the minimal effective distance $\ell = \sqrt{D_0\tau}$ to the origin, and perfect transmission. The leakage current $-\dot{Q}_{x_0} \simeq \frac{1}{2} p(t)$, where $p(t) = -\dot{P}_{\rm surv}(t; x_0 + \ell)$ is the probability density for time intervals t between successive returns to the origin. For $x_0 \ll \ell$, $p(t) \simeq \phi(t) \simeq \sqrt{\tau/4\pi}\, t^{-3/2}$ (Fig. 3b).

In general, driving the current $J_0(\omega)$, e.g. by the source $J_0(\omega)\,[\delta(x - x_0) - \delta(x + x_0)]$, results in the current $J(\omega) = \tilde{\varphi}(\omega)\, J_0(\omega)$ across the barrier for $\omega \ll D_0/x_0^2$. The "potential drop" $-\Delta\psi(\omega) \equiv J(\omega)/\kappa = Z_m(\omega) J_0(\omega)$ across the barrier is then related to $J_0(\omega)$ via the "impedance" $Z_m(\omega) = \tilde{\varphi}(\omega)/\kappa$. The excess current in the previous example is equivalent to $J_0(\omega) = \frac{1}{2}$, yielding $J(t) = \frac{1}{2} p(t)$.

Multiple barriers

Averaging over positions of randomly placed barriers with concentration n is done in a standard way1,2,10,11,28,32, by introducing the self-energy part $\Sigma_{\omega,q}$,

$$G^{-1}_{\omega,q} = G^{(0)^{-1}}_{\omega,q} - \sum\nolimits_{\omega,q}. \quad (19)$$

On the mean-field level, we keep in $\Sigma_{\omega,q}$ only the exact interaction vertex with a single barrier,

$$\sum\nolimits_{\omega,q} \simeq n \mathbf{V}_{\omega;q,q}. \quad (20)$$

The mean-field approximation is correct in the first order in barrier concentration $n = S/2V$ for all frequencies, as justified in the section on the origin of the $\sqrt{\omega}$ dispersion.

The self-energy shifts the pole of the propagator $G_{\omega,q}$, thereby changing the diffusive dynamics due to disorder-averaged interaction with random membranes. Remarkably, on this level there are no higher-order terms in powers of q^2. This allows us to represent interaction with membranes solely as renormalization of the effective diffusivity $D_0 \to \mathcal{D}(\omega)$, equation (4), which acquires frequency dependence $\tilde{\varphi}(\omega)$ dictated by that of the vertex (18). The role of $\mathcal{D}(\omega)$ is similar to that played by the dispersive refraction index. Indeed, the relation (20) is analogous to the mean-field relation between the refraction index and the

forward scattering amplitude49. In our case, the presence of "scatterers" (barriers) introduces the memory kernel (5) into the current-density response.

In higher dimensions $d > 1$, averaging is performed both over positions of the barrier in the direction **n** normal to its surface, and over its orientations. This amounts to a frequency shift $i\omega \to i\omega(\mathbf{q}) = i\omega - D_0\mathbf{q}_{||}^2$, $\Sigma_{\omega,\mathbf{q};\mathbf{n}} = (S/2V)\mathbf{V}_{\omega(\mathbf{q});\mathbf{qn},\mathbf{qn}}$, with $\mathbf{q}_{||} = \mathbf{q} - (\mathbf{qn})\mathbf{n}$ the conserved momentum parallel to the barrier, and subsequent orientational average $\Sigma_{\omega,\mathbf{q}} \equiv \langle \Sigma_{\omega,\mathbf{q};\mathbf{n}} \rangle_{\mathbf{n}}$. Substituting the latter self-energy part in equation (19), obtain the result (4) for any d.

Effective medium picture

The RG approach assumes that the boundary condition (1) is adjusted accordingly, $D_0 \to \mathcal{D}(\omega)|_L$ at each RG scale L. Strictly speaking, this is valid only for sufficiently small frequencies $\sqrt{\mathcal{D}(\omega)/\omega} \gg 1/n$, corresponding to diffusing past many membranes, when the system can be treated as a uniform effective medium at each RG step. Luckily, for the opposite case of large frequencies the full result (6) matches the exact $\sqrt{\omega\tau} \gg \zeta$ limit (4), corresponding to the original boundary condition (1). This allows us to keep the frequency simply as a parameter in equation (8).

From this discussion one expects that the agreement of the RG result (6) with the simulations to be the worst in the intermediate regime, when $\sqrt{\mathcal{D}/\omega} \sim 1/n$, equivalent to $t \sim \tau_r$. Fig. 2a shows that the discrepancy between the RG result and the simulations is indeed highest around $t \sim \tau_r$ and remains under 25%. The agreement improves for $t \gg \tau_r$ to within 10% even for the largest ζ.

We note that in $d = 1$, the RG limit $C_1(\infty)$ overestimates the exact result for the one-dimensional lattice model11,44–46, $\sqrt{2/\pi}$, by the factor of two. We also observe this in the one-dimensional simulations (not shown). There are no exact results for this problem for $d > 1$. As it is often true with mean-field-like description, the accuracy of our solution is likely to improve for increasing d. This is consistent with the notably better agreement (Fig. 2c) of the theoretically obtained coefficient $C_2(\zeta)$ with that determined from the $d = 2$ simulations.

Monte Carlo dynamics was realized on a square patch with periodic boundary conditions, embedded with randomly placed and oriented membranes, cf. Fig. 1, of nearly identical S/V in each disorder realization. For every ζ value in Fig. 2, the diffusion coefficient $D(t)$ was calculated by averaging the displacement variance $\langle x^2 \rangle$, cf. equation (3), over a total of 4×10^5 random walkers evenly split between 40 disorder realizations, with an average of 385 membranes per patch. The trajectory of each random walker was a sequence of moves in a randomly chosen direction over a distance $dr = \sqrt{4D_0 dt}$ during a time step dt, with the total diffusion time t up to 100 τ_r, corresponding to a maximum of 4×10^6 time steps per walker. Transmission across a membrane occurred with probability $P \propto \kappa dr/D_0 \ll 1$, cf. refs. 30,50. The disorder strength ζ was varied by changing κ. The time step dt for each ζ was chosen so that $P < 0.007$, and the ratio $dr/\bar{a} = Sdr/4V < 0.1$. We calibrated our results for a quasi-one-dimensional disorder (random parallel membranes), which reproduced the exact limit (2)

with about 1% accuracy. The random walk simulator was developed in C++. Simulations were performed on the NYU General Cluster. With an average of 200 CPU cores used simultaneously, all simulations took a total of about 100 hours.

Supplementary Material

Refer to Web version on PubMed Central for supplementary material.

Acknowledgments

We thank Valerij Kiselev and Daniel Sodickson for discussions. Research was supported by the Litwin Fund for Alzheimer's Research, and the National Institutes of Health Grants 1R01AG027852 and 1R01EB007656.

References

1. Haus JW, Kehr KW. Diffusion in regular and disordered lattices. Phys Rep. 1987; 150:263–406.
2. Bouchaud JP, Georges A. Anomalous diffusion in disordered media: Statistical mechanisms, models and physical applications. Phys Rep. 1990; 195:127–293.
3. Sinai YG. Dynamical systems with elastic reflections. Russ Math Survey. 1970; 25:137–189.
4. Marinari E, Parisi G, Ruelle D, Windey P. Random Walk in a Random Environment and 1/*f* Noise. Phys Rev Lett. 1983; 50:1223–1225.
5. Fisher DS. Random walks in random environments. Phys Rev A. 1984; 30:960–964.
6. Aronovitz A, Nelson DR. Anomalous diffusion in steady fluid flow through a porous medium. Phys Rev A. 1984; 30:1948–1954.
7. Fisher DS, Friedan D, Qiu Z, Shenker SJ, Shenker SH. Random walks in two-dimensional random environments with constrained drift forces. Phys Rev A. 1985; 31:3841–3845. [PubMed: 9895965]
8. Kravtsov VE, Lerner IV, Yudson VI. Random walks in media with constrained disorder. J Phys A. 1985; 18:L703–L707.
9. Lerner IV. Distributions of the diffusion coefficient for the quantum and classical diffusion in disordered media. Nucl Phys A. 1993; 560:274–292.
10. Ernst MH, Machta J, Dorfman JR, van Beijeren H. Long Time Tails in Stationary Random Media. I Theory J Stat Phys. 1984; 34:477–495.
11. Visscher PB. Universality in disordered diffusive systems: Exact fixed points in one, two, and three dimensions. Phys Rev B. 1984; 29:5472–5485.
12. Sykova E, Nicholson C. Diffusion in Brain Extracellular Space. Physiol Rev. 2008; 88:1277–1340. [PubMed: 18923183]
13. Cory DG, Garroway AN. Measurement of translational displacement probabilities by NMR: An indicator of compartmentation. Magn Reson Med. 1990; 14:435–444. [PubMed: 2355827]
14. Le Bihan, D., editor. Diffusion and Perfusion Magnetic Resonance Imaging. Raven Press; New York: 1995.
15. Callaghan, PT. Principles of Nuclear Magnetic Resonance Microscopy. Clarendon; Oxford: 1991.
16. Latour LL, Svoboda K, Mitra PP, Sotak CH. Time-dependent diffusion of water in a biological model system. Proc Nat Acad Sci USA. 1994; 91:1229–1233. [PubMed: 8108392]
17. Yablonskiy DA, et al. Quantitative *in vivo* assessment of lung microstructure at the alveolar level with hyperpolarized ^{3}He diffusion MRI. Proc Nat Acad Sci USA. 2002; 99:3111–3116. [PubMed: 11867733]
18. Friedman, MH. Principles and Models of Biological Transport. Springer; New York: 2008.
19. Fujiwara T, Ritchie K, Murakoshi H, Jacobson K, Kusumi A. Phospholipids undergo hop diffusion in compartmentalized cell membrane. J Cell Biol. 2002; 157:1071–1082. [PubMed: 12058021]
20. Kusumi A, et al. Paradigm shift of the plasma membrane concept from the two-dimensional continuum fluid to the partitioned fluid: High-speed single-molecule tracking of membrane molecules. Annu Rev Biophys and Biomol Struct. 2005; 34:351–378. [PubMed: 15869394]

21. Wawrezinieck L, Rigneault H, Marguet D, Lenne PF. Fluorescence Correlation Spectroscopy Diffusion Laws to Probe the Submicron Cell Membrane Organization. Biophys J. 2005; 89:4029–4042. [PubMed: 16199500]
22. Cotts RM. Diffusion and diffraction. Nature. 1991; 351:443–444.
23. Callaghan PT, Coy A, Macgowan D, Packer KJ, Zelaya FO. Diffraction-like effects in NMR diffusion studies of fluids in porous solids. Nature. 1991; 351:467–469.
24. Mitra PP, Sen PN, Schwartz LM, Le Doussal P. Diffusion propagator as a probe of the structure of porous media. Phys Rev Lett. 1992; 68:3555–3558. [PubMed: 10045734]
25. Mair RW, et al. Probing porous media with gas diffusion NMR. Phys Rev Lett. 1999; 83:3324–3327. [PubMed: 11543587]
26. Song YQ, Ryu S, Sen PN. Determining multiple length scales in rocks. Nature. 2000; 406:178–181. [PubMed: 10910355]
27. Sen PN. Time-dependent diffusion coefficient as a probe of the permeability of the pore wall. J Chem Phys. 2003; 119:9871–9876.
28. Altshuler, BL.; Aronov, AG. Electron-Electron Interactions in Disordered Systems. Efros, AL.; Pollak, M., editors. North-Holland; Amsterdam: 1985.
29. Scher H, Lax M. Stochastic transport in a disordered solid. I. Theory. Phys Rev B. 1973; 7:4491–4502.
30. Powles JG, Mallett MJD, Rickayzen G, Evans WAB. Exact analytic solutions for diffusion impeded by an infinite array of partially permeable barriers. Proc Roy Soc A. 1992; 436:391–403.
31. Crick F. Diffusion in Embryogenesis. Nature. 1970; 225:420–422. [PubMed: 5411117]
32. Novikov DS, Kiselev VG. Effective medium theory of a diffusion-weighted signal. NMR in Biomed. 2010; 23:682–697.
33. Warburg E. Ueber das Verhalten sogenannter unpolarisirbarer Elektroden gegen Wechselstrom. Ann Phys (Leipzig). 1899; 303:493–499.
34. Kohlrausch F. Ueber die elektromotorische Kraft Sehr Dunner Gasschichten auf Metallplatteu. Pogg Ann. 1873; 148:143–154.
35. Wien M. Ueber die Polarisation bei Wechselstrom. Ann Phys Chem. 1896; 58(294):37–72.
36. Cole KS. Alternating current conductance and direct current excitation of nerve. Science. 1934; 79:164–165. [PubMed: 17788146]
37. Cole KS, Cole RH. Dispersion and absorption in dielectrics. J Chem Phys. 1941; 9:341–351.
38. Sen PN, Scala C, Cohen MH. A self-similar model for sedimentary rocks with application to the dielectric constant of fused glass beads. Geophysics. 1981; 46:781–795.
39. Norris AN, Callegari AJ, Sheng P. A generalized differential effective medium theory. J Mech Phys Solids. 1985; 33:525–543.
40. Avellaneda M. Iterated Homogenization, Differential Effective Medium Theory and Applications. Commun Pure Appl Math. 1987; XL:527–554.
41. Abrahams E, Anderson PW, Licciardello DC, Ramakrishnan TV. Scaling Theory of Localization: Absence of Quantum Diffusion in Two Dimensions. Phys Rev Lett. 1979; 42:673–676.
42. Kosterlitz JM, Thouless DJ. Ordering, metastability and phase transitions in two-dimensional systems. J Phys C. 1973; 6:1181–1203.
43. Novikov DS, Kiselev VG. Surface-to-volume ratio with oscillating gradients. 2011; Xiv: 1101.2669. Preprint ar.
44. Denteneer PJH, Ernst MH. Diffusion in systems with static disorder. Phys Rev B. 1984; 29:1755–1768.
45. Machta J. Generalized diffusion coefficient in one-dimensional random walks with static disorder. Phys Rev B. 1981; 24:5260–5269.
46. Zwanzig R. Non-Markoffian Diffusion in a One-Dimensional Disordered Lattice. J Stat Phys. 1982; 28:127–133.
47. Sukstanskii AL, Yablonskiy DA, Ackerman JJH. Effects of permeable boundaries on the diffusion-attenuated MR signal: insights from a one-dimensional model. J Magn Reson. 2004; 170:56–66. [PubMed: 15324758]

48. Dudko OK, Berezhkovskii AM, Weiss GH. Diffusion in the presence of periodically spaced permeable membranes. J Chem Phys. 2004; 121:11283–11288. [PubMed: 15634083]
49. Landau, LD.; Lifshits, EM. Quantum Mechanics (Non-relativistic Theory). Elsevier; Oxford: 1977.
50. Fieremans E, Novikov DS, Jensen JH, Helpern JA. Monte Carlo study of a two-compartment exchange model of diffusion. NMR in Biomed. 2010; 23:711–724.

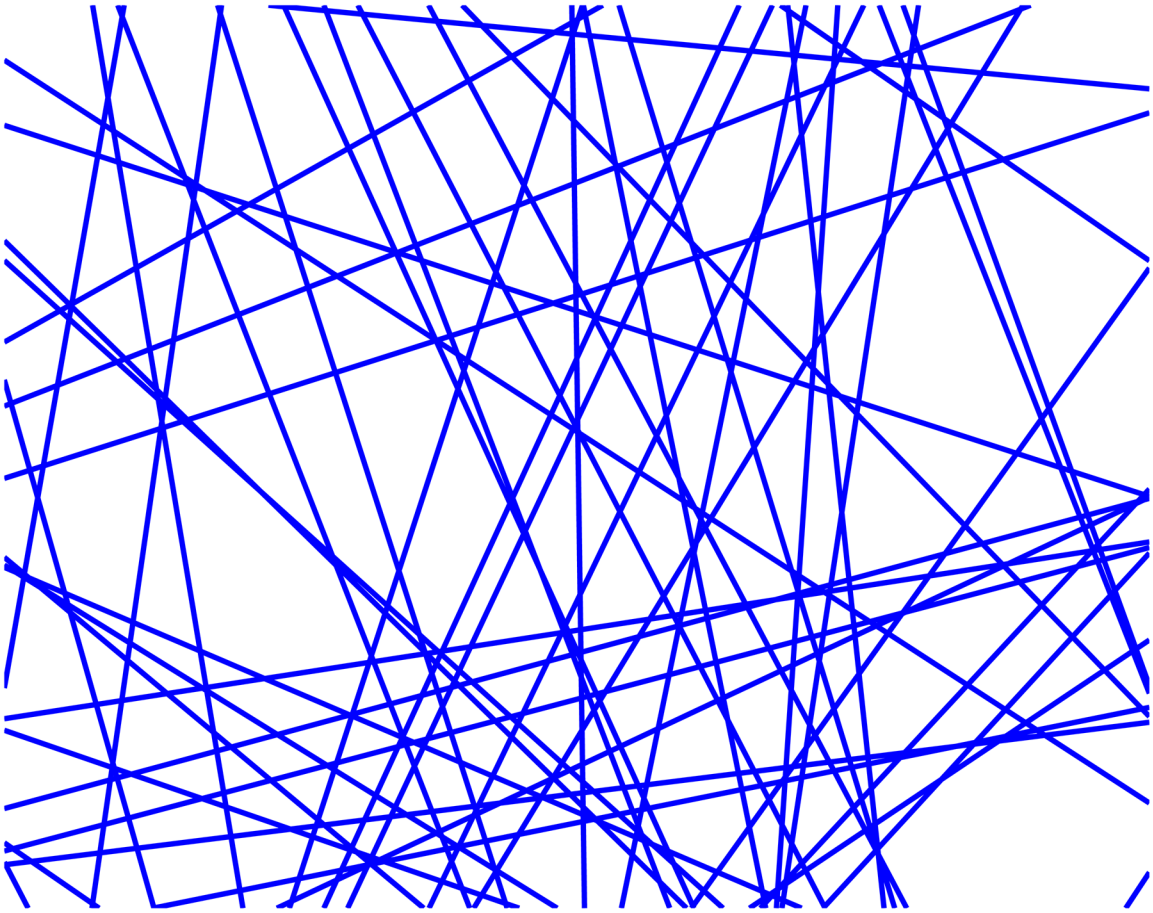

FIG. 1.

A fragment of a two-dimensional patch with randomly placed and oriented membranes (one of the disorder realizations used in the simulations).

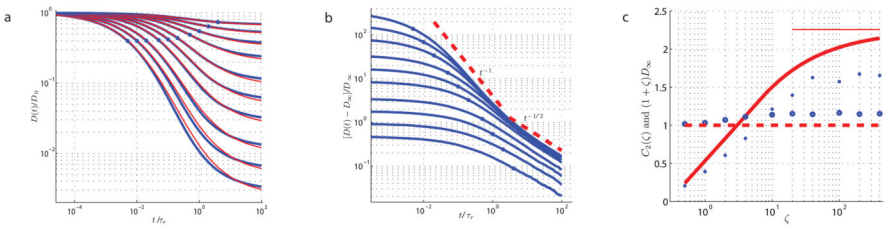

FIG. 2.

Time-dependent diffusion coefficient $D(t)$ for the two-dimensional random medium of Fig. 1. **a**, Comparison of the RG solution (6), red, with the Monte Carlo simulations, blue, for the set of decreasing permeabilities, corresponding to $\zeta = 0.5, 1, 2, 4, 10, 20, 40, 100, 200, 400$ (top to bottom). The diffusion time τ_D is marked by blue circles. **b**, Scaling behavior of $D(t)$. As the strength ζ of the restrictions increases from bottom to top, the numerical curves begin to collapse as a signature of the universal behavior (10). Dashed lines show the $\zeta \to \infty$ limits from our RG solution: the "impermeable" limit $D(t)/D_\infty = 2d\ \tau_r/t$ and the scaling limit (10) with $C_2(\infty)=4/\sqrt{\pi}$. **c**, Parameters of the scaling limit (10), $C_2(\zeta)$ (filled circles) and $D_\infty(\zeta)$ (open circles), determined from the fit of the simulations in **b** to equation (10), compared with the RG predictions (solid and dashed red lines). Thin solid line is the RG limit $C_2(\infty)=4/\sqrt{\pi}$.

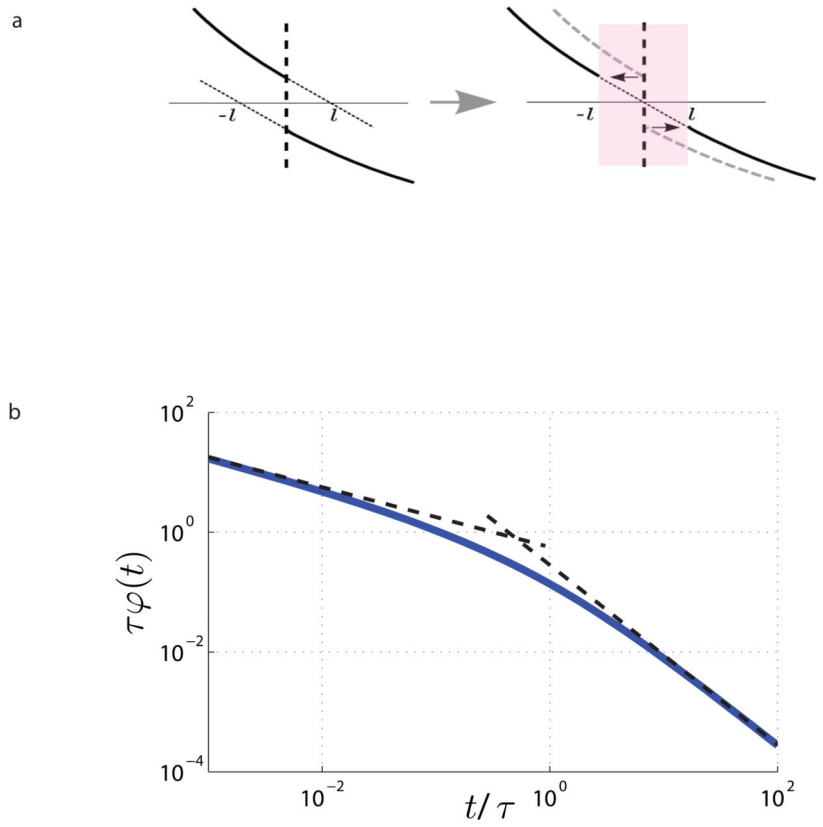

FIG. 3.

Effect of a single membrane. **a,** Meaning of effective membrane thickness: $2\ell = D_0/\kappa$ is the distance by which one should shift the density profile $\psi(x)$ on each side of membrane if one were to heal p the jump discontinuity (1). **b,** The memory kernel $\varphi(t)$, equation (5), together with its limits $\phi \simeq 1/\sqrt{\pi\tau t}$ for $t \ll \tau$, and $\phi \simeq \sqrt{\tau/4\pi}t^{-3/2}$ for $t \gg \tau$.